Title
Genomic Structure of the Mouse Ap3b1 Gene in Normal and Pearl Mice

Journal
Genomics, 69(3)

ISSN
0888-7543

Authors
Feng, Lijun
Rigatti, Brian W
Novak, Edward K
et al.

Publication Date
2000-11-01

DOI
10.1006/geno.2000.6350

Peer reviewed

Genomics **69,** 370–379 (2000)
doi:10.1006/geno.2000.6350, available online at http://www.idealibrary.com on IDEAL®

Genomic Structure of the Mouse *Ap3b1* Gene in Normal and Pearl Mice

Lijun Feng,* Brian W. Rigatti,† Edward K. Novak,*
Michael B. Gorin,†,‡ and Richard T. Swank*,[1]

*Department of Molecular and Cell Biology, Roswell Park Cancer Institute, Elm and Carlton Streets, Buffalo, New York 14263; and †Department of Ophthalmology, and ‡Department of Human Genetics, University of Pittsburgh, Pittsburgh, Pennsylvania 15213

Received May 23, 2000; accepted August 1, 2000

The mouse hypopigmentation mutant pearl is an established model for Hermansky–Pudlak syndrome (HPS), a genetically heterogenous disease with misregulation of the biogenesis/function of melanosomes, lysosomes, and platelet dense granules. The pearl (*Ap3b1*) gene encodes the β3A subunit of the AP-3 adaptor complex, which regulates vesicular trafficking. The genomic structure of the normal *Ap3b1* gene includes 25 introns and a putative promoter sequence. The original pearl (*pe*) mutation, which has an unusually high reversion rate on certain strain backgrounds, has been postulated to be caused by insertion of a transposable element. Indeed, the mutation contains a 215-bp partial mouse transposon at the junction point of a large tandem genomic duplication of 6 exons and associated introns. At the cDNA level, three pearl mutations (pearl, pearl-8J, and pearl-9J) are caused by deletions or duplications of a complete exon(s).

INTRODUCTION

The pearl mouse is an autosomal recessive hypopigmentation mutant that arose spontaneously on the C3H/HeJ background (Sarvella, 1954). It is an appropriate model for a type of inherited human albinism, Hermansky–Pudlak syndrome (HPS), as it exhibits hypopigmentation, lysosomal secretion abnormalities, and reduced levels of adenine nucleotides and serotonin in platelet dense granules (Swank *et al.*, 1998; Swank *et al.*, in press). Pearl mice also display prolonged bleeding symptomatic of platelet storage pool deficiency (SPD) (Swank *et al.*, 1998; Swank *et al.*, in press) and a significantly reduced life span (McGarry *et al.*, 1999). The pearl mouse is also a model for human congenital stationary night blindness since it has reduced sensitivity in the dark-adapted state (Balkema *et al.*, 1983; Pinto *et al.*, 1985).

HPS patients are deficient in the biosynthesis/function of melanosomes, platelet dense granules, and lysosomes (Witkop *et al.*, 1990a; King *et al.*, 1995; Shotelersuk and Gahl, 1998; Spritz, 1999). HPS causes high morbidity and increased mortality in the fourth to fifth decades of life, due to associated fibrotic lung disease, prolonged bleeding, and colitis (King *et al.*, 1995; White, 1990; Witkop *et al.*, 1990b; Shotelersuk and Gahl, 1998; Spritz, 1999). No curative therapies exist. HPS is a genetically heterogenous disease and is found in diverse populations worldwide (Hazelwood *et al.*, 1997; Oh *et al.*, 1998; Shotelersuk and Gahl, 1998; Spritz, 1999; Dell'Angelica *et al.*, 1999). This is consistent with the existence of at least 14 genetically distinct mouse pigment mutants that exhibit phenotypes similar to those of HPS patients (Swank *et al.*, 1998; Swank *et al.*, in press).

The pearl gene, now designated *Ap3b1* (Feng *et al.*, 1999), and its human orthologue *ADTB3A* (Dell'Angelica *et al.*, 1999) encode the β3A subunit of the AP-3 adaptor complex, which is involved in sorting specific membrane proteins and facilitating carrier vesicle formation at the *trans*-Golgi network (Dell'Angelica *et al.*, 1997; Simpson *et al.*, 1997). These vesicles are then targeted to their specific subcellular destinations, including lysosomes and presumably platelet dense granules and melanosomes.

The cDNA sequences of both human and mouse β3A subunit genes have been determined (Dell'Angelica *et al.*, 1997; Simpson *et al.*, 1997; Feng *et al.*, 1999). Two pearl (*pe*) mutations, a 793-bp duplication in pearl and a 107-bp deletion in pearl-8J (Feng *et al.*, 1999) and compound mutations in HPS patients (Dell'Angelica *et al.*, 1999), have been reported. These mutations lead to the depletion of the β3A subunit, which in turn results in a decrease or an abolition of other subunits of the AP-3 complex (Zhen *et al.*, 1999). Mislocalization of the entire AP-3 complex and loss of its function with subsequent defects in all three above-mentioned organelles ensue (Dell'Angelica *et al.*, 1999; Zhen *et al.*, 1999). The importance of the AP-3 complex in SPD and

[1] To whom correspondence should be addressed at Department of Molecular and Cell Biology, Roswell Park Cancer Institute, Elm and Carlton Streets, Room 245, Cell and Virus Building, Buffalo, NY 14263. Telephone: (716) 845-3429. Fax: (716) 845-8169. E-mail: Richard.Swank@RoswellPark.org.

0888-7543/00 $35.00

in the biosynthesis/function of subcellular organelles is further confirmed by organellar alterations in another HPS mouse model, mocha (Kantheti *et al.*, 1998), in *Drosophila* pigmentation mutations *garnet* (Ooi *et al.*, 1997), *carmine* (Mullins *et al.*, 1999), and *ruby* (Kretzschmar *et al.*, 2000), and in yeast (Cowles *et al.*, 1997; Stepp *et al.*, 1997).

Determination of the genomic structure of the mouse *Ap3b1* gene allows exploration of the structural basis of the original pearl mutation. This mutation is particularly interesting because it is unstable (Russell, 1964; Russell and Major, 1956). On some backgrounds, e.g., strain 201 (A^y/a), as many as 6% of *pe/pe* animals have various sized patches of normal coat color. Spontaneous revertants (pe^R/*pe*) on the congenic C57Bl/6J background also have been reported (Pinto *et al.*, 1985). It has been suggested that a transposable element may be responsible for the pearl mutation and its high reversion rate (Whitney and Lamoreux, 1982).

MATERIALS AND METHODS

Mice. Pearl and pearl-9J mutant mice together with control C3H/HeJ and C57Bl/6J mice, respectively, were obtained from The Jackson Laboratory (Bar Harbor, ME). The pearl (*pe*) mutant occurred spontaneously on the C3H/HeJ strain (Sarvella *et al.*, 1954) and has subsequently been maintained as a congenic mutant on the C57Bl/6J inbred background by repeated backcrossing. The pearl-9J (pe^{9J}) mutant occurred spontaneously on the C57Bl/6J inbred stain. Pearl revertant mice (pe^R) were originally found as a spontaneous reversion in a congenic *pe/pe* colony on the C57Bl/6J background (Pinto *et al.*, 1985) and maintained as heterozygotes (pe/pe^R). Mice were subsequently bred and maintained in the animal facilities of Roswell Park Cancer Institute (Buffalo, NY).

Primers. All primers were designed from cDNA (Feng *et al.*, 1999) or genomic sequences of the mouse *Ap3b1* gene obtained in this research using the Primer 3 program with default settings (http://www-genome.wi.mit.edu/cgi-bin/primer/primer3.cgi; Whitehead Institute). Most primers have a T_m of 60°C. These primers served for both sequencing and PCR.

Primers used to determine exon/intron boundaries are listed in Table 1. Other primers used in this study were as follows: (A) Primers derived from mouse *Ap3b1* cDNA (GenBank Accession No. AF103809): −66F, 5′-CAGCCATCCCGTAGAGGAC-3′; −40R, 5′-CTCCCGACTGCTCGTTGTA-3′; 3430F, 5′-CCACTGCTGCTGCCTTTCAT-3′; 3579R, 5′-GGTTAGCAAAGCGAGGAGG-3′. (B) Primers derived from intron sequences obtained from this study: 23F1, 5′-TAGTTTCAGACCTACGCGGG-3′; 23F2, 5′-TGGTCCACATTTGCATTTTG-3′; 23F3, 5′-GGGAGGGAGATGGTGGTAA-3′; 23F4, 5′-AACACCACCATTTGCATCAC-3′; 23F5, 5′-GCAGGGGTTAAGTTTTGCTG-3′; 23F6, 5′-ACCAAAATCTGTGGGGTCTC-3′; 23F7, 5′-TTGCTCCCAACATCTTCAAA-3′; 23F8, 5′-CCTGGGACAGACAGGAGTTC-3′; 23F9, 5′-GAAATGGGGCTGCACATAG-3′; 23R1, 5′-CTACTAGATGAGCCCCGCAG-3′; 23R2, 5′-GACCCGGCTTTCTCTAGCTT-3′; 23R3, 5′-GTTTTCAGAATGGGGAGCAG-3′; 23R4, 5′-ATGTACGTCTGGTTGAGGGG-3′; 23R5, 5′-TCTGGTCTGTTTTGTGCCAG-3′; 23R6, 5′-AGCTGAGACGAAAGGATGGA-3′; 23R7, 5′-ACAGTGTGTGGGAACAGCAG-3′; 23R8, 5′-GGATCAAACTCAGGCCTTCA-3′; 17R3, 5′-GAACCCTCACACAGGACTCG-3′.

Direct BAC sequencing. In addition to BACs described previously (Feng *et al.*, 1999), new BACs (112E17, 258F15, 127J5, 180O22, and 97J4) were isolated from the mouse BAC library RPCI 22 (http://bacpac.med.buffalo.edu/22framemouse.htm). Two BACs (112E17 and B255G14) form a minimum tiling path covering the full length of the *Ap3b1* gene sequence at the genomic level. Portions of these two BACs were directly sequenced with primers derived from the *Ap3b1* cDNA sequence (GenBank Accession No. AF103809) or the genomic sequence obtained later.

BAC DNA of these two BACs was reliably prepared with the Qiagen Midi Kit (Qiagen) according to the manufacturer's protocol with one modification: DNA was eluted at 65°C with 2.0 ml buffer QF three times. About 50 μg high-quality DNA could be reliably obtained from a total of 200 ml culture in four parallel preparations.

Sequencing was conducted with the ABI Prism 377 DNA Sequencer and the BigDye Terminator Cycle Sequencing Ready Reaction Kit from ABI Prism according to the manufacturer's protocol. Different sets of primers and templates at various ratios were tested to optimize sequencing conditions. Sequencing is optimal with 30 pmol primer and 300–1000 ng BAC DNA in a total 20-μl reaction. The thermocycling conditions were optimized from a protocol of the University of Oklahoma (http://www.genome.ou.edu/big_dyes_cos_bac_pac_fos.html) as follows: (1) 95°C for 5 min for 1 cycle; (2) 95°C for 30 s, 50°C for 20 s, 60°C for 4 min for 100 cycles; (3) maintain at 4°C. Data were analyzed by the ABI Prism Sequencing Analysis v.3.3.

PCR, PCR cloning, and sequencing. In addition to direct BAC sequencing, a vector-bubble PCR method (Riley *et al.*, 1990) was conducted to determine the exon/intron boundaries. BAC DNAs were prepared and digested with restriction enzymes. Resulting fragments were then ligated to the vectorette adaptor. PCR was performed using a specific cDNA primer and the vectorette primer. The resulting PCR products were subcloned and sequenced to determine the genomic sequence.

The Expanded Long Template PCR system or the Expand High Fidelity PCR system from Roche was used for genomic PCR amplification according to the manufacturer's protocol. PCR products were cloned by TA cloning into the pCR-XL-TOPO vector in the TOPOXL PCR cloning kit from InVitrogen according to the manufacturer's protocol. PCR products were treated with the Presequencing kit (USB) to remove excess dNTPs and primers. Products were then sequenced in a Perkin–Elmer 377 DNA sequencer using an ABI Prism BigDye Terminator Cycle Sequencing Kit according to the manufacturer's protocol.

RESULTS

Genomic Structure of the Ap3b1 Gene in Normal Mice

The genomic structure, in particular, the exon/intron boundaries, of the normal *Ap3b1* gene was determined by direct BAC sequencing and a vector-bubble PCR method (Riley *et al.*, 1990). Primers were first derived from the mouse *Ap3b1* cDNA (GenBank Accession No. AF103809), and then more primers were derived from genomic sequences obtained in this study. Primers used successfully in determining the exon/intron boundaries are listed in Table 1. A total of 25 introns were identified, and both 5′ and 3′ splice sites were sequenced. Exon/intron boundaries are presented in Table 2. Additional sequences of each intron were determined and can be accessed at GenBank (Table 2). Most exon/intron boundaries follow the GU-AG rule (Senapathy *et al.*, 1990; Shapiro and Senapathy, 1987) with one exception at the 3′ splice site of intron 2, where intron 2 ends with GC (Table 2).

The 5′ untranslated region (UTR) and 3′ UTR are about 201 and 793 bp long, respectively, and other exons range from 56 to 233 bp (Table 2). The sizes of four introns that have been determined range from 1.7 to 10.6 kb.

Possible transcription start points were determined from three different cDNA clones (unpublished data).

TABLE 1

Primers Used to Determine Exon/Intron Boundaries of the Mouse Pearl (*Ap3b1*) Gene

1F: 5′-CAGCCATCCCGTAGAGGAC-3′	1R: 5′-CAATCATCCCAACAATTCGC-3′
2F: 5′-GAGCAACAAAGATTCTGCCA-3′	2R: 5′-CAGTCGGAAGTGTGTGGTTG-3′
3F: 5′-GAAGGGGAAAAATGCCTCG-3′	3R: 5′-CGCTGGAAAGTGCTTATGG-3′
4F: 5′-CAGGACCTGGCTCTTCTGTC-3′	4R: 5′-ACAGGCACGATAATTGGCAC-3′
5F: 5′-TATCGTGCCTGTCATGATGC-3′	5R: 5′-CGTGCTCTTGTCTTTCAGAAG-3′
6F: 5′-GCAGAAGGAGATGTTAATTG-3′	6R: 5′-CCTGTGAATCAGATCGATTC-3′
7F: 5′-CCGAAAGCTTTGTAACCTGC-3′	7R: 5′-GGCATACGACTTCTTCCTGC-3′
8F: 5′-GAAACACCAAGCCGTTGC-3′	8R: 5′-CCAATATAGCTGAGCGACAGC-3′
9F: 5′-CTATATTGGCACATCTCAC-3′	10R: 5′-GATCATAGTTGGATCAGTGG-3′
11F: 5′-TGGCAAATGAAGCCAACATA-3′	11R: 5′-GTTGCACATCTGCCTATGGTC-3′
12F: 5′-GCCAGGACAAACAGTTTGC-3′	12R: 5′-GCTGCATTTGCAACAATTTC-3′
13F: 5′-GTTGTTGCTGAGAGTGTGG-3′	13R: 5′-TCCTCAAAACATCAGGAGCA-3′
14F: 5′-TGCTCCTGATGTTTTGAGGA-3′	14R: 5′-TGCGGTCTCTGATGTCGTAG-3′
15F: 5′-CGCACACGATTTATTAGGCAG-3′	15R: 5′-CAAGCTGGAAGCGATCCCTAT-3′
16F: 5′-CAGAGCAACACCTCCAAACA-3′	16R: 5′-CACTGTCACTGCTGCTATC-3′
17F: 5′-GAAGATGAGGATGAGAACCCC-3′	17R: 5′-TGGTTTTGGAGTTCCTCTTGGC-3′
18F: 5′-GCCAGAAGGTGGCCAAGAGG-3′	18R: 5′-CATGGAACTGGACTCCTCAC-3′
19F: 5′-TTTGTCTGCACAAGGGTTTG-3′	19R: 5′-TTGGAGGGAGGATGTCTTTC-3′
20F: 5′-AACCCCAGCAAGAAAGACATCC-3′	20R: 5′-ATCAAGCTTGGAGAAAGGGC-3′
21F: 5′-TTAACCCAGTATCCACCCCA-3′	21R: 5′-CTCATGTGTTTTTGTTGGCACG-3′
22F: 5′-TGCATGCCTTTCATCCAATA-3′	22R: 5′-ACTGAGACAGTCACGGACCC-3′
23F: 5′-CTCTCTGGAGCCTAAGGGGT-3′	23R: 5′-CTCTGACATGGCCACAGGT-3′
24F: 5′-GGGGTGAAGCAGAAACTCAG-3′	24R: 5′-GAGGATCATGGAGGGAGTG-3′
25F: 5′-TGAACGAGACTTCGGCTAC-3′	25R: 5′-TGTAAGCAGGTTACCCCTGG-3′

Note. F (forward) primers and R (reverse) primers were used to determine the 5′ and the 3′ splice sites, respectively, of each intron. The number before F or R designates the number of the intron whose splice sites are determined. All primers are derived from the cDNA sequence except for 2R, 16F, 19F, and 24F, which are derived from introns 3, 15, 18, and 23, respectively. Since genomic sequence obtained with primer 10R included the entire intron 10, exon 10, and the 3′ part of intron 9, primers 9R and 10F were not needed.

The longest cDNA sequence was deposited with GenBank (Feng *et al.*, 1999; GenBank Accession No. AF103809). The genomic sequence upstream of the 5′ UTR (GenBank Accession No. AF255566, Fig. 1A) of the *Ap3b1* gene was then determined by sequencing BAC 112E17 directly with primer −40R in the 5′ UTR. No apparent TATA box or initiator was found. Several stretches of GC-rich regions or putative "CpG islands," as are seen in some housekeeping genes (Smale, 1997), were found within the first 300 bp of the upstream sequence (Fig. 1A). Genomic sequence (GenBank Accession No. AF255589, Fig. 1B) following the poly(A) addition site (Barabino and Keller, 1999) was obtained by direct BAC sequencing with primer 3430F in the 3′ UTR. This sequence is required to design primers amplifying the entire 3′ UTR in mutation screening.

Tandem Genomic Duplication in the Pearl Mutation

The pearl mutation has a significant tandem duplication of 793 bp at the cDNA level (Feng *et al.*, 1999). A possible model for the origin of this duplication is a corresponding duplication at the genomic level. To test this model, genomic sequences of portions of the duplication, including two introns (introns 17 and 23) that flank the duplication, were obtained by genomic PCR and direct BAC sequencing. These analyses revealed that the pearl mutation indeed contains a tandem duplication of six entire exons (exons 18–23) and associated introns at the genomic level. The identical duplicated units (Fig. 2) are linked by a unique junction intron that retains the upstream 5.6 kb of the 3′ intron (intron 23) and downstream 1.6 kb of the 5′ intron (intron 17), which are separated by a 0.2-kb partial mouse transposon (MT) (Heinlein *et al.*, 1986) at the junction point. A more detailed description of the 5′, 3′, and junction introns follows.

The 5′ Intron of the Pearl Duplication

Primers 17F and 17R (Fig. 2A), which are located in exons 17 and 18, respectively, were used to amplify the 5′ intron of the pearl duplication. PCR products of 2.6 kb from genomic DNA of normal C3H/HeJ, pearl, and pearl revertant mice were cloned and sequenced. A 2558-bp intron (intron 17, GenBank Accession No. AF255582) was revealed. No sequence differences were found between C3H/HeJ, pearl, and pearl revertant mice within this intron.

In this intron, two pentanucleotide repeat sequences, $(CAAAA)_7$ (nt 425–459, numbering from the first nt of intron 17) and $(TTTTG)_7$ (nt 698–732), separated by 230 bp, were found (Fig. 3A). They could perfectly match to form a hairpin structure. Also a partial *Alu*-like sequence of 134 bp (nt 753–886) was found 15 bp 3′ to the $(TTTTG)_7$ repeats (Fig. 3A).

The 3′ Intron of the Pearl Duplication

Primers from exons 23 and 24, which flank the 3′ intron, were used to amplify the entire 3′ intron by genomic PCR. However, all primer sets failed due to

TABLE 2

Exon/Intron Boundaries of the Pearl (*Ap3b1*) Gene

Exon No.	GenBank Accession No.	Terminal nt[a]/size (bp)	5′ Splice site EXON/intron	Intron No.	Intron size (kb)	3′ Splice site intron/EXON
1	AF255566	(128/201)	GGAAGAA**gt**gagga	1	?	gtaat**ag**GAATGAA
2	AF255567	(212/85)	TGATTGC**gt**tccag	2	?	tgatt**gc**GAAGGGG
3	AF255568	(279/68)	CATCGAG**gt**aatgt	3	?	caaat**ag**ATCAAGA
4	AF255569	(375/97)	TTTGAAG**gt**aaatc	4	?	gttttagGACCCGA
5	AF255570	(536/162)	TGTACAG**gt**gggtg	5	?	attct**ag**TCTTGAC
6	AF255571	(603/68)	GAGCACG**gt**gagcg	6	?	ttctt**ag**CTGGTGG
7	AF255572	(786/184)	GAGAGAG**gt**gagtt	7	?	ctyct**ag**GATGGTG
8	AF255573	(945/160)	TGCAGCG**gt**acgtg	8	?	tttcc**ag**GTGGTTA
9	AF255574	(1043/99)	GCAATAG**gt**aggtc	9	?	cttct**ag**GGAGGTG
10	AF255575	(1098/56)	GAGAAAG**gt**atgta	10	?	cacccagGGTATGT
11	AF255576	(1233/136)	ATTTCAG**gt**ttgca	11	?	ttttt**ag**ACCTACG
12	AF255577	(1366/134)	AGGGATG**gt**gagtt	12	?	cttttagAAATAGT
13	AF255578	(1476/111)	TATCACT**gt**gagtg	13	?	gtatt**ag**GTTCCTG
14	AF255579	(1653/178)	CAAACAG**gt**aagas	14	1.7	cgaac**ag**ACAAAAT
15	AF255580	(1840/188)	TTTAAAG**gt**atcac	15	?	ttaat**ag**ATAGGGA
16	AF255581	(1971/132)	AGAGTCA**gt**aagtt	16	?	taaac**ag**GCAAAAG
17	AF255582	(2134/164)	GACAGTG**gt**gggct	17	2.6	cttgc**ag**AGAGCGG
18	AF255582	(2282/149)	GGAAAAG**gt**aacga	18	?	tttac**ag**TGATTCA
19	AF255583	(2430/149)	GGCTCCG**gt**aagac	19	?	cttac**ag**GCAAAAG
20	AF255584	(2504/75)	GACGACT**gt**aagtt	20	?	cttct**ag**TTAACCC
21	AF255585	(2610/107)	CATCAAC**gt**aagtg	21	?	tgccc**ag**GTCAGTA
22	AF255586	(2842/233)	CCAATAG**gt**aaagg	22	3.8	ttctt**ag**ACTCTCT
23	AF255587	(2927/86)	AATTGTG**gt**aagtt	23	10.6	tcctt**ag**CACCAAG
24	AF255587	(3025/99)	GAGCAAG**gt**gagag	24	?	gttgc**ag**GAACGCT
25	AF255588	(3164/140)	TACACAG**gt**agtct	25	?	tttgc**ag**GTTTGCA
26	AF255589	(3956/793)	GAATAGC[b]atttgcc			

[a] Terminal nt of each exon, numbering from the start codon of *Ap3b1* cDNA (AF103809).
[b] Poly(A) addition site.

the 10.7-kb length of this intron. Therefore overlapping portions of a BAC (B255G14, Feng *et al.*, 1999) from mouse strain 129 were sequenced directly. Primers 23F and 23R, located in exons 23 and 24, respectively (Fig. 2), were first used to obtain partial 5′ and 3′ sequences of the 3′ intron. Then a series of nine primers (23F1 to 23F9), located within the 5′ portion of the intron and oriented toward the 3′ end, plus another 8 primers (23R1 to 23R8), located within the 3′ portion of the intron and oriented toward the 5′ end, were designed (Fig. 2A). These primers were used in direct BAC sequencing to obtain more genomic sequence by walking. The entire 10.7-kb normal intron sequence was thus determined. PCR primers were then designed to amplify overlapping parts of the entire intron from C3H/HeJ, pearl, or pearl revertant mice. Complete sequencing of the 3′ intron (GenBank Accession No. AF255587) of C3H/HeJ, pearl, and pearl revertant mice revealed no sequence differences.

A partial LINE1 element of 869 bp (nt 6542–7410, numbering from the first nt of intron 23) and a partial *Alu*-like sequence of 75 bp (nt 2321–2395) were found in the 3′ intron (Fig. 3B). This partial *Alu*-like sequence is in opposite orientation to the 134-bp partial *Alu* sequence found in the 5′ intron and has 83% (62/75) identity. No other significant sequence similarity was found between the 5′ and the 3′ introns.

A

AGCGCGAACAATCTAGCGCACCGGGAGCGGCAGGCGCGGGCCCGCACGGACACA
GTGCGCACGCGCAGGGGGTGGGCCGCCCGGTCAGCCGGAGCAGTGACGAGCCCG
GAAGCGCCGGCGCGCGCCCCCTCCGCCCCAGAACTAGTTTGGTTCGGTGTCCTC
CGAACGCCAGCCATCCGTAGAGGACCCCGCACGCTCTCTCCCGCACCCGCCTGC
TGGCCAGCACCGCCCGCG**ATG**TCTAGCAACAGTTTCGCCTACAACGAGCAG

B

AGGTAAATAAAGGAGTATATGAATAG**C**ATTTGCCTCTCCTAATCCTTACTGGC
TGAACTTTCTTTGTTCCAAAATATTTCTGGTCACACTGTGGAGAAACTTCTCCC

FIG. 1. Genomic sequences of the mouse *Ap3b1* gene, including a putative promoter sequence and the sequence following the poly(A) site, obtained by direct BAC sequencing. (**A**) Sequence of the putative *Ap3b1* gene promoter and part of the 5′ UTR. The start codon (ATG) is in boldface type. Putative CpG island sequences are underlined. (**B**) Genomic sequence following the poly(A) site. The poly(A) signal is underlined, and the poly(A) addition site, determined by cDNA clone sequences, is in boldface type and in a larger font.

Junction Intron in the Pearl Mutation

According to the duplication model (Fig. 2), the junction intron is flanked by exons 23 and 18. Primers (23F and 17R) were thus paired to amplify the entire junction intron. A 7.4-kb product was obtained only from pearl DNA, not from wildtype C3H/HeJ or C57Bl/6J DNA, and the entire junction intron sequence (GenBank Accession No. AF267848) was obtained. As predicted, the junction intron has bona fide partial sequences of the 3′ intron (5558 bp, nt 1–5558, numbering from the first nt of the junction intron, Fig. 3) and the 5′ intron (1619 bp, nt 5777–7395, Fig. 3).

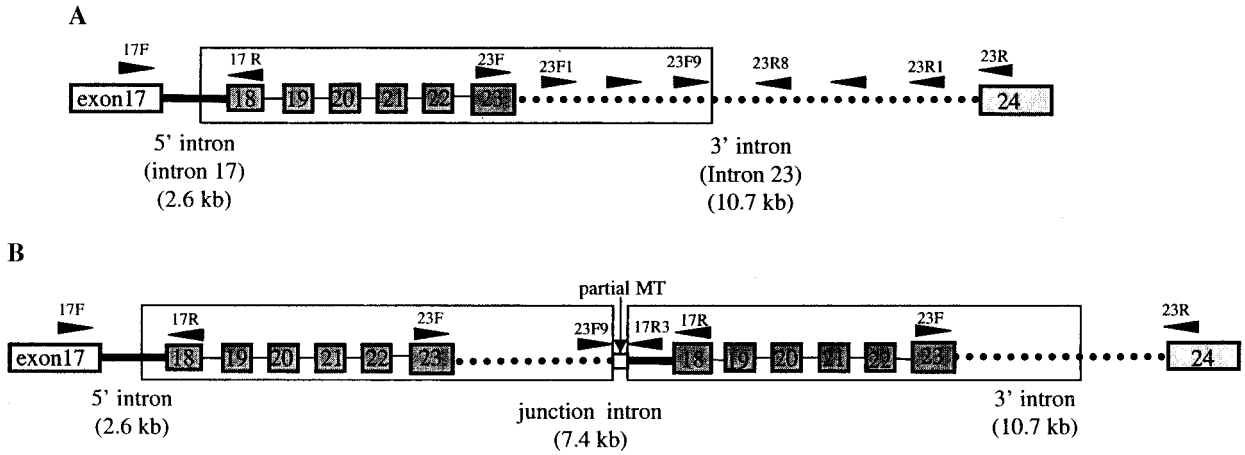

FIG. 2. Tandem duplication of a portion of the *Ap3b1* gene in pearl mice. (**A**) Structure of the *Ap3b1* gene in normal mice. The region that is duplicated in pearl mice (**B**) is enclosed within the large box. (**B**) Exons 18–23 together with associated introns, including portions of introns 17 and 23, are duplicated in the pearl mutation. Exons are depicted as numbered boxes. 5′ and 3′ introns are depicted as straight and dotted heavy lines, respectively, and other introns are depicted as thin lines (not drawn to scale). Arrows represent primers, pointing in the 5′ to 3′ direction. The partial MT is presented as a small box in the junction intron and is indicated by an arrow. The duplicated units are enclosed within large boxes.

The breakpoints in both 5′ and 3′ introns are readily identified. In addition, a 218-bp (nt 5559–5776, Fig. 3C) foreign DNA sequence was found between the two duplicated regions. With the exception of the first 3 bp (AAA), this foreign sequence is part of the internal sequence of a 1.2-kb retrovirus-like element termed MT (Heinlein *et al.*, 1986), which is a subgroup of the mammalian apparent LTR-retrotransposons (MaLRs) (Smit, 1993).

This partial MT sequence was compared with a full-length MT (Fig. 4). It is 97% identical to the full-length MT over the 215 bp. There are two 9-nt direct repeats (GAAAAATTG) flanking this partial MT (Fig. 3C). The 5′ repeat contains 3 bp (GAA) of the 3′ intron sequence, 3 bp (AAA) of foreign sequence of unknown origin, and 3 bp (TTG) of the partial MT sequence (Fig. 3C). On the other hand, the 3′ repeat is derived entirely from the 5′ intron sequence (Fig. 3C). This repeat sequence has no homology to the consensus 5-bp (AAAGG) insertion target site of the MaLR family (Smit, 1993). A BLAST search in GenBank found partial or full-length MT sequences in the mouse genome (GenBank Accession Nos. AC003062, AC004407, AC005403, AC005816, etc). However, no such 9-nt direct repeats were found at their ends.

The Pearl Revertant Allele (pe^R) Produces a Normal Transcript of the Ap3b1 Gene

Pearl revertant mice were maintained as heterozygotes (*pe/pe*^{R}). The exact genotype was first investigated by genomic PCR. A set of primers (23F9 and 17R3, Fig. 2B) that amplifies specifically the junction point of the pearl duplication was used. As expected, a

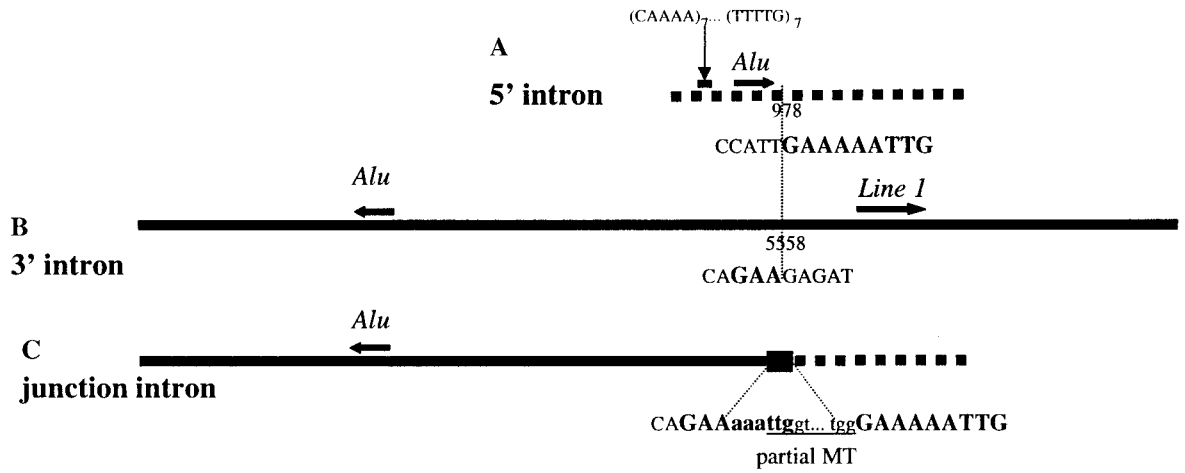

FIG. 3. Detailed structures of the (**A**) 5′, (**B**) 3′, and (**C**) junction introns in pearl (*pe*) mice. *Alu*-like, LINE1 sequences, and a hairpin structure ($(CAAAA)_7 \ldots (TTTTG)_7$) are labeled. Breakpoints (vertical dotted line) in the 5′ and 3′ introns are numbered. Partial sequences at the breakpoints are given underneath. In **C,** sequences derived from the 5′ and 3′ introns are given in uppercase letters; sequence derived from the partial mouse transposon (MT) is in lowercase letters and is underlined. The complete sequence of the partial MT is given in Fig. 4. The repeat sequences flanking the partial MT in C are in boldface type.

```
   1 taaacccttt cctccccaac ttgcttcttg gtcatgatgt ttgtgcagga atagaaaccc
  61 tgactaagac aaattggtac cagcagagtg gggtattcct gtgacaacct gaccatgttc
 121 tggggaggat tgtggaagga ctttggaact ttgggcttga agatccattc gttgttaaga
 181 gctctgtcag atgttgtgta ggagcttgga agataatgtt gagaacagtg cagaagatgg
 241 aggtttggtt tgtgaaattt cagagggaaa attaaagact cttttcaggg ccattgctgc
 301 tttgattgtg aagattctgt agttctggtt agctggggct gaagaatcag ctgtgattaa
 361 caagatacca gaactactaa agcaaaaact ttgcattact gggactattg atgctggtta
 421 gctggagcta agaaattagc ggtgattaag aagagaccag catcattgag gtgacatctt
 481 ctgggaggtg ttttctgaga gcacagtggc tgtgttccag atatagccaa agttgtacct

 541 tgtgctgtgg ctggacttgg taatgtgtaa gagtcaccca ggtggtactg gttttgaagg
Partial MT        AAA•••• •••C•••••• •••••••••• •••••••••• ••••••••••
 601 catgaaggag ttgagcagaa cagctgaggc ttggcactgt gagaggccat ggaaggccat
     •••••••••A •••••••••G ••• •••••• •••••••••• •••••••••• ••••••••••
 661 tggtgaaagt gcagcctcag ttgcaattga tggcccagga ctgaaggggt catgcagtgt
     •••••••••• •••••••••• •••••••••• •••••••••• •••••••••• ••••••••••
 721 tttggagatg ccagtaccat gagatgacca ccaagagcag cagcagcagt ggagtacagg
     •••••••••• •••••••••• •••••••••• •••••••••• •••••••••• •

 781 cgtctggagc ctacaggatg acacatgtgc tacaaagggc ctggctggag aagtgatcca
 841 agcccttgga ggagcccaga agatcgtgag ttggatccca gacattggac ggttagagat
 901 tgacttttgc ttttgattgt gactgtgccc tgatattttc cctcttgaag gaagaaactg
 961 ttttagtgga gcccacagtt aagagacttt taattgtaaa aagactttgg attttaaaag
1021 agatggatat tttaaagaga ttgaaatttt aagcatatgt aaagactgtg ggacttttaa
1081 agttatttag aatggggatg aataagattg taagggttga ggcttactag tgatgtgttt
1141 gtgtgtcaag ttgacaaggg gtcaattgta ctggctagct ttgtgtcaac ttgacacagc
1201 tggagttatc acagagaaag gagcttca
```

FIG. 4. Comparison of the 215-bp partial MT sequence found at the junction point of the pearl duplication with a full-length (1227 bp) MT (GenBank Accession No. U17089). The full-length MT sequence is given in lowercase letters. LTRs (bp 1–71 and 1166–1227) of the full-length MT sequence are underlined. The 218-bp partial MT insertion sequence is given underneath the full-length MT sequence with identical sequences indicated by dots and different sequences by uppercase letters.

product of 678 bp was obtained from pearl (*pe/pe*), heterozygous pearl (*pe/+*), and pearl revertant (pe/pe^R) mice but not from wildtype C3H/HeJ mice (Fig. 5A), establishing the presence of the pearl allele (*pe*) in the first three genotypes. Primer sets that amplify the entire 5′ and 3′ introns were also used. These products are expected to be a mixture of products from both *pe* and pe^R alleles from the heterozygous pearl revertant mice. However, sequences of these products showed no heterogeneity and no sequence differences between wildtype, pearl, and pearl revertant mice (data not shown). Therefore it is not possible to differentiate the pe^R allele from either the wildtype or the *pe* allele by the genomic PCR method.

The sequence identity between the pe^R allele and the wildtype alleles and the fact that the pearl revertant mice display normal coat color suggested that the pearl revertant allele (pe^R) represented a reversion to wildtype. To test this possibility, RT-PCR was conducted to study transcripts of the pearl (*pe*) and the pearl revertant (pe^R) alleles in the heterozygous pearl revertant (pe/pe^R) mouse. RNA was isolated from kidneys of normal, pearl (*pe/pe*), heterozygous pearl (*pe/+*), and pearl revertant (pe/pe^R) mice and a pair of primers (−66F and 3579R) was used to amplify the entire coding region of the *Ap3b1* gene. As expected, a product of 3.7 kb from the wildtype allele was apparent in the C3H/HeJ mice, while there was a 4.4-kb product from the *pe* allele in pearl (*pe/pe*) mice. In heterozygous pearl (*pe/+*) mice, both products were observed (Fig. 5B). Likewise, in the pearl revertant mice, both the 4.4-kb product of the *pe* allele and the 3.7-kb product of the pe^R allele were observed (Fig. 5B). Sequencing of the 3.7-kb RT-PCR product from the pearl revertant mice revealed that the transcript of the pe^R allele is identical to the wildtype *Ap3b1* cDNA. It is thus concluded that the pearl revertant allele (pe^R) produces a normal transcript of the *Ap3b1* gene.

The greater amount of the 3.7-kb product in the pe^R and wildtype alleles than of the 4.4-kb product in the *pe* allele (Fig. 5B) is probably due to (1) less mutant than normal transcript due to rapid degradation of the mutant transcript and/or (2) preferential amplification of the shorter product in RT-PCR.

A trivial explanation for the reversion, i.e., a contamination of a C57Bl/6J wildtype allele in our mouse colony, has been excluded. Genotyping of microsatellite markers closely surrounding the *pe* locus in pearl revertant mice revealed they are homozygous for C3H/HeJ (data not shown), the original background of the pearl mutation (Sarvella, 1954). Similarly, a contamination of a wildtype C3H/HeJ allele has been excluded, because the distant genetic markers *D13Mit13* and *D13Mit30,* which flank the *pe* locus, and *D17Mit79,* which is on chromosome 17, are homozygous C57Bl/6J type (data not shown), as expected for the congenic

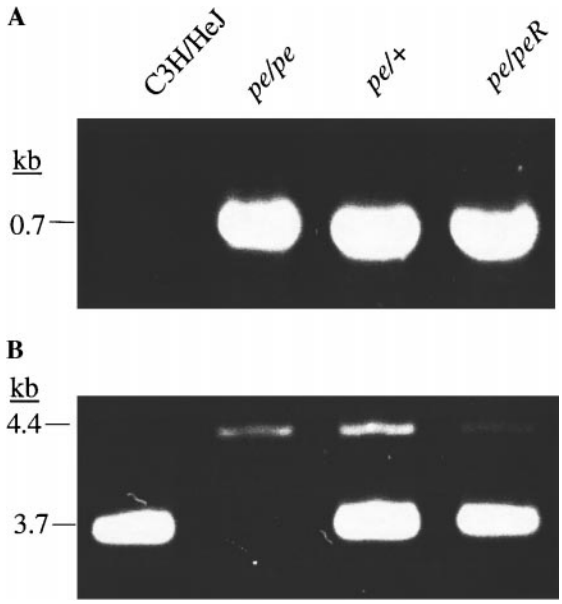

FIG. 5. The pearl revertant mouse is heterozygous for the *pe* and *peR* alleles. PCR amplifications were conducted using samples from C3H/HeJ, *pe/pe, pe/+*, and *pe/peR* mice. (**A**) Genomic PCR product specific for the *pe* duplication (amplified with primers 23F9 and 17R3; Fig. 2B) is present in pearl revertant mice. (**B**) RT-PCR product of the *peR* allele (3.7 kb, amplified with primers −66F and 3579R) from pearl revertant mice is the same size as the wildtype allele.

strain. In addition, C3H/HeJ contamination would have produced an immediately recognizable *agouti* phenotype rather than the black color of the pearl revertants.

Mutations in Three Pearl Alleles All Involve Large Deletions or Duplications of an Entire Exon(s) at the cDNA Level

Mutations in two pearl alleles, a 793-bp duplication in pearl and a 107-bp deletion in pearl-8J, were determined previously at the cDNA level (Feng *et al.*, 1999). In this study an 867-bp in-frame deletion in the 5′ part of the *Ap3b1* transcript was found in another pearl mutation, pearl-9J, by RT-PCR. This deletion, from nt 787 to 1653 (numbering from the start codon, GenBank Accession No. AF103809), is predicted to result in a deletion of 289 amino acids, which is approximately 1/3 of the normal protein product. Such a large deletion likely produces unstable and/or nonfunctional mRNA and/or protein as was found in other pearl mutations (Feng *et al.*, 1999). Indeed, the β3A subunit was not detected by Western blotting using a polyclonal antibody (Simpson *et al.*, 1997) in kidney of pearl-9J mice (data not shown).

Analyses of the exon/intron boundaries (Table 2) revealed that all mutations found in the above three pearl alleles involve precise deletions or duplications of a complete exon(s). The pearl-9J deletion spans seven exons, exons 8–14 of 867 bp; the pearl-8J deletion includes one exon, exon 20 of 107 bp; and the original pearl duplication includes 6 exons, exon 18–23 of 793 bp. A set of primers targeting the junction region of intron 20 and exon 21 amplified a product of the expected size from normal mice but not from the pearl-8J mice (data not shown), suggesting a deletion at the genomic level as well. The 5′ splice site of intron 7 and the 3′ splice site of intron 14 were compared between the pearl-9J and its normal control mice. No sequence differences were found (data not shown).

DISCUSSION

Genomic Structure of the Mouse Ap3b1 Gene

A total of 25 introns were found in the mouse *Ap3b1* gene. All the exon/intron boundaries were determined (Table 2), most of which follow the GU-AG rule (Shapiro and Senapathy, 1987) with only one exception. Intron 2 ends with a GC rather than a conserved AG. GC at the 3′ splice site is rare but is present in both rodents and primates (Senapathy *et al.*, 1990; Jackson, 1991). These results will be useful for determination of the genomic structure of the human β3A gene.

Conserved promoter elements like TATA boxes or initiators were not apparent in the promoter region sequence obtained by direct BAC sequencing using a primer in the 5′ UTR. Instead, several putative CpG islands were found within the 300 bp upstream of the 5′ UTR (Fig. 1A). These may serve as regulatory elements as has been reported for some housekeeping genes (Smale, 1997). Genomic sequence following the 3′ UTR was also obtained by direct BAC sequencing with a primer in the 3′ UTR and should prove useful in amplification and sequencing of the entire 3′ UTR.

Recently, HPS patients with compound heterozygous mutations in the *HPS2* gene were reported (Dell'Angelica *et al.*, 1999). A method to screen additional HPS patients for mutations in this gene would be useful. Though RT-PCR is advantageous, a genomic PCR-based protocol will be useful in those cases for which only genomic DNA samples are available. Since the mouse *Ap3b1* gene and human *HPS2* gene share a high level of homology at the cDNA level, the genomic structures of the two genes are expected to be similar, and some primers used here may likewise amplify corresponding human sequences.

Pearl Duplication

One reason for determining the genomic structure of the *Ap3b1* gene was to investigate the nature of the pearl genomic mutation, which has an unusually high reversion rate (Russell, 1964; Russell and Major, 1956). The pearl mutation was previously determined to be a tandem duplication at the cDNA level (Feng *et al.*, 1999). By genomic sequencing, we have demonstrated that the pearl mutation is also a large tandem duplication at the genomic level. As we proposed, the pearl mutation has two identical segments containing all six exons (18–23) and associated introns (Fig. 2). These two segments are linked by a junction intron

that maintains the 5′ 5.6 kb of the 3′ intron and the 3′ 1.6 kb of the 5′ intron. In addition, a 218-bp foreign sequence, including a 215-bp partial MT (Heinlein *et al.*, 1986), was found at the junction point of the duplication.

Mouse transposons are a subgroup of a superfamily of MaLRs (Smit, 1993), which resemble the internal sequences of the human transposon-like element (Paulson *et al.*, 1985). The 215-bp partial MT sequence (Fig. 4) is a part of the internal MT sequence that has no homology to any other proteins or long terminal repeats and has no special significance in the evolution of the MT (A. Smit, La Jolla, pers. comm., 28 Mar. 2000).

The mechanism for formation of the pearl duplication and the exact role of the MT in the duplication are not clear. Tandem duplications involving a portion of a single gene have been reported for a number of genes (Hu and Worton, 1992; Deininger and Batzer, 1999). Two general mechanisms leading to such tandem duplications have been proposed: homologous and nonhomologous recombination (Hu and Worton, 1992; Purandare and Patel, 1997; Lambert *et al.*, 1999). Homologous recombination occurs between a stretch of homologous sequences, like *Alu* repeats (Gondo *et al.*, 1993; Deininger and Batzer, 1999; Lambert *et al.*, 1999). In these cases, the breakpoints and junction points are usually located within homologous sequences. Though two partial *Alu*-like sequences were found in the 5′ and 3′ introns (Fig. 3), they are in opposite orientation and thus cannot produce a tandem duplication by the usual homologous recombination models (Hu and Worton, 1992; Purandare and Patel, 1997; Lambert *et al.*, 1999). No other significant homologies were found at the breakpoints of 5′ or 3′ introns or the junction points. In another model (Hu and Worton, 1992; Roth *et al.*, 1985), duplications are created by nonhomologous recombination upon random chromatid cleavage and rejoining events. This mechanism is the most likely cause of the pearl duplication. It is possible that the insertion of the MT introduces a chromatid break in either the 5′ or the 3′ intron, followed by a nonhomologous recombination event that results in duplication and partial loss of the MT. It has long been proposed that the pearl mutation may be due to the insertion of a transposable element (Whitney and Lamoreux, 1982). The location of the partial MT precisely at the junction point is consistent with this model. The pearl mutation is nevertheless not simply due to an insertion of a transposable element, but is rather a complicated large tandem duplication at the genomic level. Also, at the cDNA level, this partial MT does not interrupt splicing or introduce mutations other than the duplication. It is also possible that insertion of the MT is irrelevant to the duplication though the probability of two such simultaneous independent events seems low.

The 9-bp direct repeats at both ends of the partial MT are of special interest. However, no such 9-bp repeat sequences were found at the ends of other full or partial MT elements found by BLAST search in GenBank. It is possible that these 9-bp direct repeats were generated by the insertion of this partial MT through a rare retrotransposition event (Lodish *et al.*, 1995) or resulted from DNA repair during chromatid rejoining events.

Pearl Reversion

Both somatic and germline reversions of the pearl mutation have been reported (Russell and Major, 1956; Russell, 1964). Although the somatic reversion events in the pearl mouse are very intriguing, this phenomenon could not be studied at this time, because no DNA or RNA samples from somatic revertants are available. Our resource was limited to frozen tissues of heterozygous pearl revertants, which are offspring of one of the two spontaneous germline revertants on the congenic C57Bl/6J background (Pinto *et al.*, 1985). These mice represent germline reversion events as the coat color is entirely normal and fully transmittable to offspring over many generations.

The revertants were maintained as heterozygotes. The nonavailability of samples from homozygous revertant (pe^R/pe^R) mice caused some technical difficulties in this study. Though we could test the presence of the *pe* allele in the revertant mice by genomic PCR with a set of primers specific for the junction point in the *pe* allele (Fig. 5A), we could not directly test the presence of the pe^R allele because no primer sets used in genomic PCR could differentiate the pe^R allele from the *pe* allele in heterozygous pearl revertant (pe/pe^R) mice. However, we could infer from the phenotype of revertant mice that the pe^R allele corrects the light coat color by reverting to the wildtype and producing a normal transcript. This was confirmed by RT-PCR (Fig. 5B). Sequencing data conclusively indicated that the pearl revertant allele produces the normal transcript.

The RT-PCR data strongly suggest that the pearl genomic duplication was lost by one mutant homologue and that it reverted to the normal wildtype structure. If the pe^R allele left some "footprints," such as a portion of the partial MT, at the breakpoints in either 5′ or 3′ intron, genomic PCR products from the pearl revertant mice would be a mixture of two products: one from the wildtype allele and another from the pe^R allele. However, we did not detect any heterogeneity of these products by sequencing. Rather, the sequences are uniformly identical to the wildtype sequences. This indicated that the pe^R allele reverted back to the wildtype with complete fidelity, at least at the 5′ and 3′ introns, though the entire genomic segment was not studied completely. This apparent exact loss of one duplicated unit (Fig. 2) in revertant mice strongly suggests an involvement of homologous recombination between two duplicated regions in the reversion process, similar to that postulated in the pink-eyed unstable

(p^{un}) (Gondo *et al.*, 1993; Schiestl *et al.*, 1997) and *HPRT* (Helleday *et al.*, 1998; Yang *et al.*, 1988) reversions. Tandem repeats are known to be highly unstable in both prokaryotes (Feschenko and Lovett, 1998) and mammals (Schiestl *et al.*, 1997). There are several models to explain the deletion of one copy of a duplication by homologous recombination such as that observed in p^{un} (Schiestl *et al.*, 1997). In any model, recombination could occur within the duplicated unit to restore the wildtype sequence arrangement, consistent with our finding of sequence identity between DNA from wildtype mice and DNA from revertant mice.

The pearl mutation is stable in its original strain, C3H/HeJ (Russell and Major, 1956). However, when transferred to other backgrounds, both somatic and germline reversions occurred. The frequency is as high as 6% on the 210 (A^y/a) strain and less on other strains (Russell, 1964). On the C57Bl/6J background, the reversion rate is about 0.5% (Pinto *et al.*, 1985). The reasons for the strain-dependent nature of the reversion rate in pearl are not clear. Presumably *trans*-acting factors that differentiate among these strains contribute.

Other Pearl Mutations

It is interesting to note that all three pearl alleles that have been studied involve substantial deletions (pearl-8J and pearl-9J) or a duplication (pearl) of a complete exon(s) at the cDNA level. The genomic nature of the former two alleles was not precisely determined. Limited data suggest that both deletions in cDNAs of pearl-8J and pearl-9J are likely due to large deletions at the genomic level as well.

ACKNOWLEDGMENTS

We thank Diane Poslinski and Debra Tabaczynski for mouse care. We thank Belinda Harris at The Jackson Laboratory's Mouse Mutant Resource for providing the pearl mutant mouse. This research was supported by NIH Grants HL31698 and EY12104 to R. T. Swank, the Mark Diamond Research Fund of SUNY at Buffalo to Lijun Feng, grants from (1) the Eye & Ear Foundation of Pittsburgh (Pittsburgh, PA), (2) Research to Prevent Blindness (New York, NY) and (3) NEI RO1-EY90912 to M. Gorin; Grant RR01183 to The Jackson Laboratory, and Roswell Park Cancer Institute Cancer Center Grant CA16056.

REFERENCES

Balkema, G. W., Mangini, N. J., and Pinto, L. H. (1983). Discrete visual defects in pearl mutant mice. *Science* **219:** 1085–1087.

Barabino, S. M., and Keller, W. (1999). Last but not least: Regulated poly(A) tail formation. *Cell* **99:** 9–11.

Cowles, C. R., Odorizzi, G., Payne, G. S., and Emr, S. D. (1997). The AP-3 adaptor complex is essential for cargo-selective transport to the yeast vacuole. *Cell* **91:** 109–118.

Deininger, P. L., and Batzer, M. A. (1999). *Alu* repeats and human disease. *Mol. Genet. Metab.* **67:** 183–193.

Dell'Angelica, E. C., Mullins, C., and Bonifacino, J. S. (1999). AP-4, a novel protein complex related to clathrin adaptors. *J. Biol. Chem.* **274:** 7278–7285.

Dell'Angelica, E. C., Ooi, C. E., and Bonifacino, J. S. (1997). β3A-adaptin, a subunit of the adaptor-like complex AP-3. *J. Biol. Chem.* **272:** 15078–15084.

Feng, L., Seymour, A. B., Jiang, S., To, A., Peden, A. A., Novak, E. K., Zhen, L., Rusiniak, M. E., Eicher, E. M., Robinson, M. S., Gorin, M. B., and Swank, R. T. (1999). The beta3A subunit gene (*Ap3b1*) of the AP-3 adaptor complex is altered in the mouse hypopigmentation mutant pearl, a model for Hermansky–Pudlak syndrome and night blindness. *Hum. Mol. Genet.* **8:** 323–330.

Feschenko, V. V., and Lovett, S. T. (1998). Slipped misalignment mechanisms of deletion formation: Analysis of deletion endpoints. *J. Mol. Biol.* **276:** 559–569.

Gondo, Y., Gardner, J. M., Nakatsu, Y., Durham-Pierre, D., Deveau, S. A., Kuper, C., and Brilliant, M. H. (1993). High-frequency genetic reversion mediated by a DNA duplication: The mouse pink-eyed unstable mutation. *Proc. Natl. Acad. Sci. USA* **90:** 297–301.

Hazelwood, S., Shotelersuk, V., Wildenberg, S. C., Chen, D., Iwata, F., Kaiser-Kupfer, M. I., White, J. G., King, R. A., and Gahl, W. A. (1997). Evidence for locus heterogeneity in Puerto Ricans with Hermansky–Pudlak syndrome. *Am. J. Hum. Genet.* **61:** 1088–1094.

Heinlein, U. A., Lange-Sablitzky, R., Schaal, H., and Wille, W. (1986). Molecular characterization of the MT-family of dispersed middle-repetitive DNA in rodent genomes. *Nucleic Acids Res.* **14:** 6403–6416.

Helleday, T., Arnaudeau, C., and Jenssen, D. (1998). A partial *hprt* gene duplication generated by non-homologous recombination in V79 Chinese hamster cells is eliminated by homologous recombination. *J. Mol. Biol.* **279:** 687–694.

Hu, X., and Worton, R. G. (1992). Partial gene duplication as a cause of human disease. *Hum. Mutat.* **1:** 3–12.

Jackson, I. J. (1991). A reappraisal of non-consensus mRNA splice sites. *Nucleic Acids Res.* **19:** 3795–3798.

Kantheti, P., Qiao, X., Diaz, M. E., Peden, A. A., Meyer, G. E., Carskadon, S. L., Kapfhamer, D., Sufalko, D., Robinson, M. S., Noebels, J. L., and Burmeister, M. (1998). Mutation in AP-3 delta in the mocha mouse links endosomal transport to storage deficiency in platelets, melanosomes, and synaptic vesicles. *Neuron* **21:** 111–122.

King, R. A., Hearing, V. J., Creel, D. J., and Oetting, W. S. (1995). Albinism. *In* "Metabolic Basis of Inherited Disease" (C. R. Scriver, A. L. Beaudet, W. S. Sly, and D. Valle, Eds.), pp. 4353–4392, McGraw-Hill, New York.

Kretzschmar, D., Poeck, B., Roth, H., Ernst, R., Keller, A., Porsch, M., Strauss, R., and Pflugfelder, G. O. (2000). Defective pigment granule biogenesis and aberrant behavior caused by mutations in the *Drosophila* AP-3 beta Adaptin gene *ruby*. *Genetics* **155:** 213–223.

Lambert, S., Saintigny, Y., Delacote, F., Amiot, F., Chaput, B., Lecomte, M., Huck, S., Bertrand, P., and Lopez, B. S. (1999). Analysis of intrachromosomal homologous recombination in mammalian cell, using tandem repeat sequences. *Mutat. Res.* **433:** 159–168.

Lodish, H., B. D., Berk, A., Zipursky, S., Matsudaira, P., and Darnell, J. (1995). "Molecular Cell Biology," 3rd ed., p. 338, Scientific American, New York.

McGarry, M. P., Reddington, M., Novak, E. K., and Swank, R. T. (1999). Survival and lung pathology of mouse models of Hermansky–Pudlak syndrome and Chediak–Higashi syndrome. *Proc. Soc. Exp. Biol. Med.* **220:** 162–168.

Mullins, C., Hartnell, L. M., Wassarman, D. A., and Bonifacino, J. S. (1999). Defective expression of the mu3 subunit of the AP-3 adaptor complex in the *Drosophila* pigmentation mutant carmine. *Mol. Gen. Genet.* **262:** 401–412.

Oh, J., Ho, L., Ala-Mello, S., Amato, D., Armstrong, L., Bellucci, S., Carakushansky, G., Ellis, J. P., Fong, C. T., Green, J. S., Heon, E., Legius, E., Levin, A. V., Nieuwenhuis, H. K., Pinckers, A., Tamura, N., Whiteford, M. L., Yamasaki, H., and Spritz, R. A. (1998). Mutation analysis of patients with Hermansky–Pudlak syndrome: A frameshift hot spot in the HPS gene and apparent locus heterogeneity. *Am. J. Hum. Genet.* **62:** 593–598.

Ooi, C. E., Moreira, J. E., Dell'Angelica, E. C., Poy, G., Wassarman, D. A., and Bonifacino, J. S. (1997). Altered expression of a novel adaptin leads to defective pigment granule biogenesis in the *Drosophila* eye color mutant garnet. *EMBO J.* **16:** 4508–4518.

Paulson, K. E., Deka, N., Schmid, C. W., Misra, R., Schindler, C. W., Rush, M. G., Kadyk, L., and Leinwand, L. (1985). A transposon-like element in human DNA. *Nature* **316:** 359–361.

Pinto, L. H., Williams, M. A., Suzuki, H., Mangini, N., Balkema, G. W., Jr., and Vanable, J. W., Jr. (1985). Visual defects in mouse hypopigmentation mutants. *Neurosci. Res. Suppl.* **2:** S239–251.

Purandare, S. M., and Patel, P. I. (1997). Recombination hot spots and human disease. *Genome Res.* **7:** 773–786.

Riley, J., Butler, R., Ogilvie, D., Finniear, R., Jenner, D., Powell, S., Anand, R., Smith, J. C., and Markham, A. F. (1990). A novel, rapid method for the isolation of terminal sequences from yeast artificial chromosome (YAC) clones. *Nucleic Acids Res.* **18:** 2887–2890.

Roth, D. B., Porter, T. N., and Wilson, J. H. (1985). Mechanisms of nonhomologous recombination in mammalian cells. *Mol. Cell. Biol.* **5:** 2599–2607.

Russell, L. (1964). Genetic and functional mosaicism in the mouse. *In* "Role of Chromosomes in Development" (M. Locke, Ed.), pp. 153–181, Academic Press, New York.

Russell, L. B., and Major, M. H. (1956). A high rate of somatic reversion in the mouse. *Genetics* **4:** 658.

Sarvella, P. A. (1954). Pearl, a new spontaneous coat and eye color mutation in the house mouse. *J. Hered.* **45:** 19–20.

Schiestl, R. H., Aubrecht, J., Khogali, F., and Carls, N. (1997). Carcinogens induce reversion of the mouse pink-eyed unstable mutation. *Proc. Natl. Acad. Sci. USA* **94:** 4576–4581.

Senapathy, P., Shapiro, M. B., and Harris, N. L. (1990). Splice junctions, branch point sites, and exons: Sequence statistics, identification, and applications to genome project. *Methods Enzymol.* **183:** 252–278.

Shapiro, M. B., and Senapathy, P. (1987). RNA splice junctions of different classes of eukaryotes: Sequence statistics and functional implications in gene expression. *Nucleic Acids Res.* **15:** 7155–7174.

Shotelersuk, V., and Gahl, W. A. (1998). Hermansky–Pudlak syndrome: Models for intracellular vesicle formation. *Mol. Genet. Metab.* **65:** 85–96.

Simpson, F., Peden, A. A., Christopoulou, L., and Robinson, M. S. (1997). Characterization of the adaptor-related protein complex, AP-3. *J. Cell Biol.* **137:** 835–845.

Smale, S. T. (1997). Transcription initiation from TATA-less promoters within eukaryotic protein-coding genes. *Biochim. Biophys. Acta* **1351:** 73–88.

Smit, A. F. (1993). Identification of a new, abundant superfamily of mammalian LTR-transposons. *Nucleic Acids Res.* **21:** 1863–1872.

Spritz, R. A. (1999). Multi-organellar disorders of pigmentation: Intracellular traffic jams in mammals, flies and yeast. *Trends Genet.* **15:** 337–340.

Stepp, J. D., Huang, K., and Lemmon, S. K. (1997). The yeast adaptor protein complex, AP-3, is essential for the efficient delivery of alkaline phosphatase by the alternative pathway to the vacuole. *J. Cell Biol.* **139:** 1761–1774.

Swank, R. T., Novak, E. K., McGarry, M. P., Rusiniak, M. E., and Feng, L. (1998). Mouse models of Hermansky Pudlak syndrome: A review. *Pigment Cell Res.* **11:** 60–80.

Swank, R. T., Novak, E. K., McGarry, M. P., Yuke, Z., Li, W., Zhang, Q., and Feng, L. Abnormal vesicular trafficking in mouse models of Hermansky–Pudlak syndrome. *Pigment Cell Res.*, in press.

White, J. G. (1990). Structural defects in inherited and giant platelet disorders. *Adv. Hum. Genet.* **19:** 133–234.

Whitney, J. B. D., and Lamoreux, M. L. (1982). Transposable elements controlling genetic instabilities in mammals. *J. Hered.* **73:** 12–18.

Witkop, C. J., Almadovar, C., Pineiro, B., and Babcock, M. N. (1990a). Hermansky–Pudlak syndrome (HPS): An epidemiologic study. *Ophthalmic Paed. Genet.* **11:** 245–250.

Witkop, C. J., Babcock, M. N., Rao, G. H. R., Gaudier, F., Summers, C. G., Shanahana, F., Harmaon K.R., Townsend, D., Sedano, H. O., and King, R. A. (1990b). Albinism and Hermansky–Pudlak syndrome in Puerto Rico. *Bol. Assoc. Med. P.R.* **82:** 333–339.

Yang, T. P., Stout, J. T., Konecki, D. S., Patel, P. I., Alford, R. L., and Caskey, C. T. (1988). Spontaneous reversion of novel Lesch–Nyhan mutation by HPRT gene rearrangement. *Somat. Cell. Mol. Genet.* **14:** 293–303.

Zhen, L., Jiang, S., Feng, L., Bright, N. A., Peden, A. A., Seymour, A. B., Novak, E. K., Elliott, R., Gorin, M. B., Robinson, M. S., and Swank, R. T. (1999). Abnormal expression and subcellular distribution of subunit proteins of the AP-3 adaptor complex lead to platelet storage pool deficiency in the pearl mouse. *Blood* **94:** 146–155.